

TResNet: High Performance GPU-Dedicated Architecture

Tal Ridnik Hussam Lawen Asaf Noy Itamar Friedman Emanuel Ben Baruch Gilad Sharir

DAMO Academy, Alibaba Group

{tal.ridnik, hussam.lawen, asaf.noy, itamar.friedman, emanuel.benbaruch, gilad.sharir}
@alibaba-inc.com

Abstract

Many deep learning models, developed in recent years, reach higher ImageNet accuracy than ResNet50, with fewer or comparable FLOPS count. While FLOPs are often seen as a proxy for network efficiency, when measuring actual GPU training and inference throughput, vanilla ResNet50 is usually significantly faster than its recent competitors, offering better throughput-accuracy trade-off.

In this work, we introduce a series of architecture modifications that aim to boost neural networks' accuracy, while retaining their GPU training and inference efficiency. We first demonstrate and discuss the bottlenecks induced by FLOPs-optimizations. We then suggest alternative designs that better utilize GPU structure and assets. Finally, we introduce a new family of GPU-dedicated models, called TResNet, which achieve better accuracy and efficiency than previous ConvNets.

Using a TResNet model, with similar GPU throughput to ResNet50, we reach 80.8% top-1 accuracy on ImageNet. Our TResNet models also transfer well and achieve state-of-the-art accuracy on competitive single-label classification datasets such as Stanford cars (96.0%), CIFAR-10 (99.0%), CIFAR-100 (91.5%) and Oxford-Flowers (99.1%). They also perform well on multi-label classification and object detection tasks. Implementation is available at: <https://github.com/mrT23/TResNet>.

1. Introduction

The seminal ResNet models [8], introduced in 2016, revolutionized the world of deep learning. ResNet models use repeated well-designed residual blocks, allowing training of very deep networks to high accuracy while maintaining high GPU utilization. ResNet models are also easy to train, and converge fast and consistent even with plain SGD optimizer [43]. NVIDIA Volta tensor cores [25] further improved ResNet models GPU utilization, up to qua-

drupling their GPU throughput on mixed-precision training and inference [42]. Among the ResNet models, ResNet50 established himself as a prominent model in terms of speed-accuracy trade-off, and became a leading backbone model for many computer vision tasks [6, 19, 40, 12].

Since ResNet50, new deep learning models were developed, which achieve better ImageNet accuracy with fewer or comparable FLOPs. Surprisingly, even though most deep learning models are trained, and sometimes deployed, on GPUs, few models try explicitly to find an optimal design in terms of GPU throughput. Since FLOPs are not an accurate proxy for GPU speed [1], sub-optimal design for GPUs might occur. This is especially true for GPU training speed, which is rarely measured and documented in academic literature, and can be severely hindered by some modern architecture design tricks [24].

Table 1 compares ResNet50 to popular newer architectures, with similar top-1 ImageNet accuracy - ResNet50-D [9], ResNeXt50 [41], SEResNeXt50 [11], EfficientNet-B1 [35] and MixNet-L [36]. We see from Table 1 that the reduction of FLOPs and the usage of new tricks in modern networks, compared to ResNet50, is not translated to improvement in GPU throughput. This is especially evident for GPU training speed, where ResNet50 gives by a large margin better speed-accuracy trade-off. We identify two main reasons for this throughput gap:

1. Modern networks like EfficientNet, ResNeXt and MixNet do extensive usage of depthwise and 1x1 convolutions, that provide significantly fewer FLOPs than 3x3 convolutions. However, GPUs are usually limited by memory access cost and not by number of computations, especially for low-FLOPs layers. Hence, the reduction in FLOPs is not translated well to an equivalent increase in GPU throughput [24].
2. Modern networks like ResNeXt and MixNet do extensive usage of multi-path. For training, this creates lots of activation maps that need to be stored for backward propagation, which reduces the maximal possible batch size, thus hurting the GPU throughput. Multi-path also limits the ability to do

Model	Top Training Speed (img/sec)	Top Inference Speed (img/sec)	Top-1 Accuracy [%]	Flops [G]
ResNet50 [8]	805	2830	79.0	4.1
ResNet50-D [9]	600	2670	79.3	4.4
ResNeXt50 [41]	490	1940	79.4	4.3
EfficientNetB1 [35]	480	2740	79.2	0.6
SEResNeXt50 [35]	400	1770	79.9	4.3
MixNet-L [36]	400	1400	79.0	0.5
TResNet-M	730	2930	80.8	5.5

Table 1. **Comparison of ResNet50 to top modern networks, with similar top-1 ImageNet accuracy.** All measurements were done on Nvidia V100 GPU with mixed precision. For gaining optimal speeds, training and inference were measured on 90% of maximal possible batch size. Except TResNet-M, all the models’ ImageNet scores were taken from the public repository [39], which specialized in providing top implementations for modern networks. Except EfficientNet-B1, which has input resolution of 240, all other models have input resolution of 224.

inplace operations [31], and can lead to network fragmentation [24].

Following Table 1, We want to design a new family of networks, TResNet, aimed at high accuracy while maintaining high GPU utilization. TResNet models will contain the latest published design tricks available, along with our own novelties and optimizations. Unlike previous works, which measure only the FLOPS proxy or just GPU inference speed, we will directly focus on both GPU inference and training speed. For a proper comparison to previous models, one network variant (TResNet-M) is designed to match ResNet50 GPU throughput, while the rest match modern larger architectures.

We will show that for all tested datasets, TResNets offer an improved speed-accuracy trade-off. Specifically, they reach ImageNet top1-accuracy of 80.8% with GPU throughput similar to ResNet50 (79.0%), and top-1 accuracy of 84.3% with better GPU throughput than EfficientNet-B5 (83.7%). Besides ImageNet, TResNets also achieve state-of-the-art accuracy on 3 out of 4 widely used downstream single-label datasets, with x8-15 faster GPU inference speed. They also excel on multi-label classification and object detection tasks.

2. TResNet Design

TResNet design is based on the classical ResNet50 architecture, with dedicated refinements, modifications and optimizations. We have three variants of TResNet: TResNet-M, TResNet-L and TResNet-XL. The three models vary only in depth and the number of channels.

TResNet architecture contains the following refinements to plain ResNet50 design:

- SpaceToDepth Stem
- Anti-Alias Downsampling
- In-Place Activated BatchNorm

- New Block-type Selection
- Optimized SE Layers.

While previous works usually offer refinements to ResNet50 where every refinement increases the accuracy at the cost of reducing the GPU throughput [9, 18, 11], in our design some refinements increase the models’ throughput, and some decrease it. All-in-all, for TResNet-M we chose a mixture of refinements that provide a similar GPU throughput to ResNet50, for fair comparison of the models’ accuracy.

2.1. Refinements

SpaceToDepth Stem - Most neural networks start with a stem unit - a component whose goal is to quickly reduce the input resolution. ResNet50 stem is comprised of a stride-2 conv7x7 followed by a max pooling layer [8], which reduces the input resolution by a factor of 4 ($224 \rightarrow 56$). ResNet50-D stem design [9], for comparison, is more elaborate - the conv7x7 is replaced by three conv3x3 layers. The new ResNet50-D stem design did improve accuracy, but at a cost of lowering the training throughput - see Table 1, where the new stem design is responsible for almost all the decline in the training throughput.

We wanted to create a fast, seamless stem layer, with little information loss as possible, and let the simple well-designed residual blocks do all the actual processing work. The stem sole functionality should be to downscale the input resolution to match the rest of the architecture, e.g., by a factor of 4. We met these goals by using a dedicated SpaceToDepth transformation layer [32], that rearranges blocks of spatial data into depth. The SpaceToDepth transformation layer is followed by simple 1x1 convolution to match the number of wanted channels, as can be seen in Figure 1.

Anti-Alias Downsampling (AA) - [44] proposed to replace all downscaling layers in a network by an equivalent

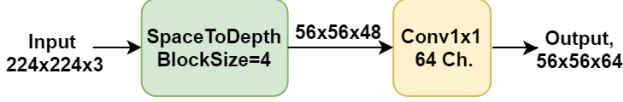


Figure 1. TResNet-M stem design.

AA component, to improve the shift-equivariance of deep networks and give better accuracy and robustness.

We implemented an economic variant of AA, similar to [18], that provides an improved speed-accuracy tradeoff - only our stride-2 convolutions are replaced by stride-1 convolutions followed by a 3x3 blur kernel filter with stride 2, as described in Figure 2.

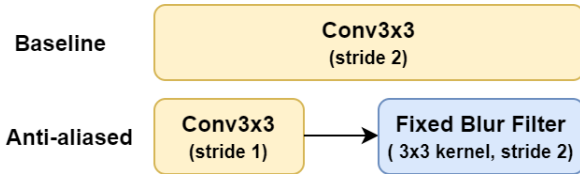


Figure 2. The AA downsampling scheme of TResNet architecture. All stride-2 convolutions are replaced by stride-1 convolutions, followed by a fixed downsampling blur filter [44].

In-Place Activated BatchNorm (Inplace-ABN) - Along the architecture, we replaced all BatchNorm+ReLU layers by Inplace-ABN [31] layers, which implements BatchNorm with activation as a single inplace operation, allowing to reduce significantly the memory required for training deep networks, with a negligible increase in computational cost. As an activation function for the Inplace-ABN, we chose to use Leaky-ReLU instead of ResNet50’s plain ReLU.

Using Inplace-ABN in TResNet models offers the following advantages:

- BatchNorm layers are major consumers of GPU memory. Replacing BatchNorm layers with Inplace-ABN enables to practically double the maximal possible batch size, which improves the GPU throughput
- For TResNet models, Leaky-ReLU provides better accuracy than plain ReLU. While some modern activation, like Swish and Mish [26], might also give better accuracy than ReLU, their GPU memory consumption is higher, as well as their computational cost. In contrast, Leaky-ReLU has exactly the same GPU memory consumption and computational cost as plain ReLU.
- The increased batch size can also improve the effectiveness of popular algorithms like triplet loss [17] and momentum-contrastive learning. [7]

Block-Type Selection - ResNet34 and ResNet50 share the same architecture, with one difference: ResNet34 uses solely ‘BasicBlock’ layers, which comprise of two conv3x3 as the basic building block, while ResNet50 uses ‘Bottleneck’ layers, which comprise of two conv1x1 and one conv3x3 as the basic building block [8]. Bottleneck layers have higher GPU usage than BasicBlock layers, but usually give better accuracy.

For TResNet models, we found that using a mixture of BasicBlock and Bottleneck layers gives the best speed-accuracy tradeoff. Since BasicBlock layers have larger receptive field, they are usually more effective at the beginning of a network. Hence, we placed BasicBlock layers at the first two stages of the network, and Bottleneck layers at the last two stages. Compared to ResNet50, we also modified the number of channels and the depth of the 3rd stage for the different TResNet models. Full specification of TResNet networks, including block type, width and number depth of each stage, appears in Table 2.

Optimized SE Layers - We added dedicated squeeze-and-excitation [11] layers (SE) to TResNet architecture. In order to reduce the computational cost of the SE blocks, and gain the maximal speed-accuracy benefit, we placed SE layers only in the first three stages of the network. Compared to standard SE design [11], TResNet SE placement and hyper-parameters are also optimized: For Bottleneck units we added the SE module after the conv3x3 operation, with reduction factor of 8, and for BasicBlock units we added SE module just before the residual sum, with reduction factor of 4. The complete blocks design, with SE layers and Inplace-ABN, is presented in Figure 3.

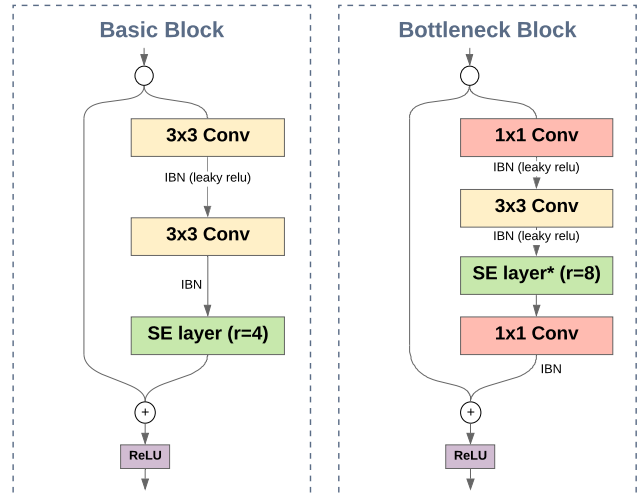


Figure 3. TResNet BasicBlock and Bottleneck design (stride 1). IBN = Inplace-BatchNorm, r = reduction factor, * - Only for 3rd stage.

Layer	Block Type	Output	Stride	TResNet					
				M		L		XL	
				Repeats	Channels	Repeats	Channels	Repeats	Channels
Stem	SpaceToDepth Conv1x1	56×56	-	1	48	1	48	1	48
			1	1	64	1	76	1	84
Stage1	BasicBlock+SE	56×56	1	3	64	4	76	4	84
Stage2	BasicBlock+SE	28×28	2	4	128	5	152	5	168
Stage3	Bottleneck+SE	14×14	2	11	1024	18	1216	24	1344
Stage4	Bottleneck	7×7	2	3	2048	3	2432	3	2688
Pooling	GlobalAvgPool	1×1	1	1	2048	1	2432	1	2688
#Params.				29.4M		54.7M		77.1M	

Table 2. Overall architecture of the three TResNet models.

2.2. Code Optimizations

We designed TResNet using the popular PyTorch [28] package. We find that PyTorch enables easy code prototyping and debugging, while remaining efficient and fast on GPUs. In this section, we will describe some code optimizations we did to enhance the GPU throughput and reduce the memory footprint of TResNet models. While code optimizations are sometimes overlooked and seen as ‘implementation details’, we claim that they are crucial for designing a modern network with top GPU performance.

2.2.1 JIT Compilation

PyTorch default option is to run code dynamically, via a Pythonic interpreter. Instead, PyTorch JIT script compilation (`torch.jit.script`) [29] enables to pre-compile certain parts of a network to C++, which can lead to various optimizations and improved performance, both during training and inference. We used JIT compilations for network modules that don’t contain learnable parameters - the AA blur filter and the SpaceToDepth modules. For modules without learnable parameters, JIT compilation is a seamless process that accelerates the network GPU throughput without imposing limitations on the actual training and inference - for example, the input size does not need to be fixed and pre-determined, flow control statements are still possible.

For the AA and SpaceToDepth modules, we found that JIT compilation reduces the GPU cost by almost a factor of two. The module’s JIT code appears in appendix A.

2.2.2 Inplace Operations

In PyTorch, inplace operations change directly the content of a given tensor, without making a copy. They reduce the memory access cost of an operation, and also prevent creation of unneeded activation maps for backward propagation, hence increasing the maximal possible batch size. In TResNet code, inplace operations are used as much as possible. All TResNet BatchNorms are done inplace

(Inplace-ABN), and there are also inplace operations for the residual connection, SE layers, blocks’ final activation and more. This is a key factor in enabling large batch size - TResNet-M maximal batch size is almost twice of ResNet50 - 512, as can be seen in Table 1. For full review of TResNet inplace operations, see the public code.

2.2.3 Fast Global Average Pooling

Global average pooling (GAP) is used heavily in TResNet architecture - both in the SE layers, and before the final fully connected.

PyTorch has two boilerplate methods for GAP - `AdaptiveAvgPool2d` and `AvgPool2d`. While `AvgPool2d` is the fastest among the two, it is still a general function, designed for many cases and usages, and not optimized for the specific case of TResNet - fixed GAP with stride 1: $(C, H, W) \rightarrow (C, 1, 1)$.

We found that a simple dedicated implementation of GAP, using PyTorch `View` and `Mean` tensor operations, can be up to 5 times faster than `AvgPool2d` on GPU. Our TResNet implementation for Fast GAP appears in appendix A.

3. ImageNet Results

In this section, we will evaluate TResNet models on standard ImageNet training (input resolution 224), and compare their top-1 accuracy and GPU throughput to other known models. We will also perform an ablation study to better understand the effect of different refinements, show results for fine-tuning TResNet to higher input resolution, and do a thorough comparison to EfficientNet models.

3.1. Basic Training

Our main benchmark for evaluating TResNet models is the popular ImageNet dataset [16]. We trained the models on input resolution 224, for 300 epochs, using a SGD optimizer and 1-cycle policy [33]. For regularization, we

used Auto-augment [4], Cutout [5], Label-smooth [34] and True-weight-decay [23]. We found that the common ImageNet statistics normalization [18, 4, 35] does not improve the training accuracy, and instead normalized all the RGB channels to be between 0 and 1. For comparison, we repeated the same training procedure for ResNet50. Results appear in Table 3.

Models	Top Training Speed (img/sec)	Top Inference Speed (img/sec)	Max Train Batch Size	Top-1 Acc. [%]
ResNet50	805	2830	288	79.0
TResNet-M	730	2930	512	80.8
TResNet-L	345	1390	316	81.5
TResNet-XL	250	1060	240	82.0

Table 3. **TResNet models accuracy and GPU throughput on ImageNet, compared to ResNet50.** All measurements were done on Nvidia V100 GPU, with mixed precision. All models are trained on input resolution of 224.

We can see from Table 3 that TResNet-M, which has similar GPU throughput to ResNet50, has significantly higher validation accuracy on ImageNet (+1.8%). It also outperforms all the other models that appear in Table 1, both in terms of GPU throughput and ImageNet top-1 accuracy.

Note that our ResNet50 ImageNet accuracy, 79.0%, is significantly higher than the accuracy stated in previous articles [8, 9, 13], demonstrating the effectiveness of our training procedure. In addition, training TResNet-M and ResNet50 models takes less than 24 hours on an 8xV100 GPU machine, showing that our training scheme is also efficient and economical.

Another strength of the TResNet models, as reflected by Table 3, is the ability to work with significantly larger batch sizes than previous models. In general, large batch size leads to better GPU utilization, and allows easier scaling to large inputs. For distributed learning, it also reduces the number of synchronization needed in an epoch between the different GPUs.

3.2. Ablation Study

We performed an ablation study to investigate the impact of the different refinements in TResNet-M model on the validation accuracy, and the model inference speed. Results appear in Table 4.

We can see from Table 4 that in terms of contribution to top-1 accuracy, SE layers and AA are the most dominate refinements, but with a price of reducing the model throughput. We were able to compensate for this decrease with refinements like SpaceToDepth stem, Inplace-ABN and new

block-type selection, that in addition to increasing to top-1 accuracy, actually improve the throughput.

Refinement	Top-1 Accuracy	Inference speed (img/sec)
Original ResNet50	79.0	2830
+ Stem \rightarrow SpaceToDepth	79.1	2950
+ Block-type selection	79.4	3320
+ Inplace-ABN	79.5	3470
+ Optimizer SE layers	80.3	3280
+ AA	80.8	2930

Table 4. **Ablation study** - The impact of refinements in TResNet-M model on ImageNet top-1 accuracy and inference speed.

3.3. High-Resolution Fine-Tuning

We tested the scaling of TResNet models to higher input resolutions on ImageNet. We used the pre-trained TResNet models that appear in Table 3 as a starting point, and did a short 10 epochs fine-tuning to input resolution of 448. The results appear in Table 5.

Model	Input Resolution	Top-1 Accuracy [%]
TResNet-M	224	80.8
TResNet-M	448	83.2
TResNet-L	224	81.5
TResNet-L	448	83.8
TResNet-XL	224	82.0
TResNet-XL	448	84.3

Table 5. **Impact of the input resolution on the top1 ImageNet accuracy for TResNet models.** All TResNet 448 input-resolution accuracies are obtained with 10 epochs of fine-tuning.

We see from Table 5 that TResNet models scale well to high resolutions. Even TResNet-M, which is a relatively small and compact model, can achieve top-1 accuracy of 83.2% on ImageNet with high-resolution input. TResNet largest variant, TResNet-XL, achieves 84.3% top-1 accuracy on ImageNet.

3.4. Comparison to EfficientNet Models

EfficientNet models, which are based on MobilenetV3 architecture [10], propose to balance the resolution, height, and width of a base network for generating a series of larger networks. They are considered state-of-the-art architectures, that provide efficient networks for all ImageNet top-1 accuracy spectrum [35]. In Figure 4 and Figure 5, we compare the inference and training speed of TResNet models to the different EfficientNet models respectively.

Top-1 Accuracy [%] Vs Inference Speed

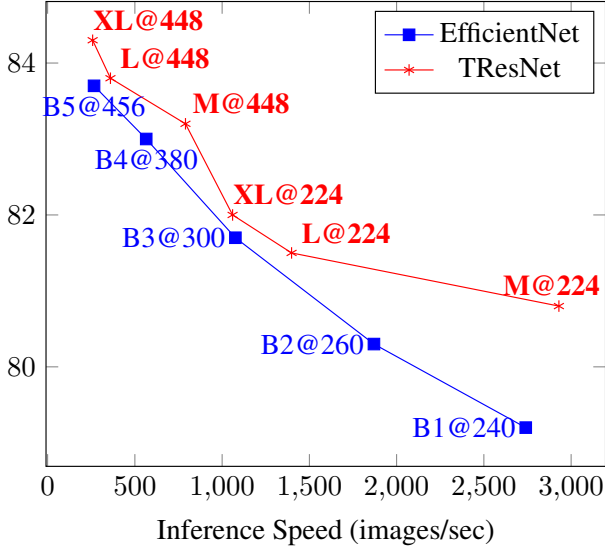


Figure 4. TResNet Vs EfficientNet models inference speed comparison. Y label is the accuracy[%]

Top-1 Accuracy [%] Vs Training Speed

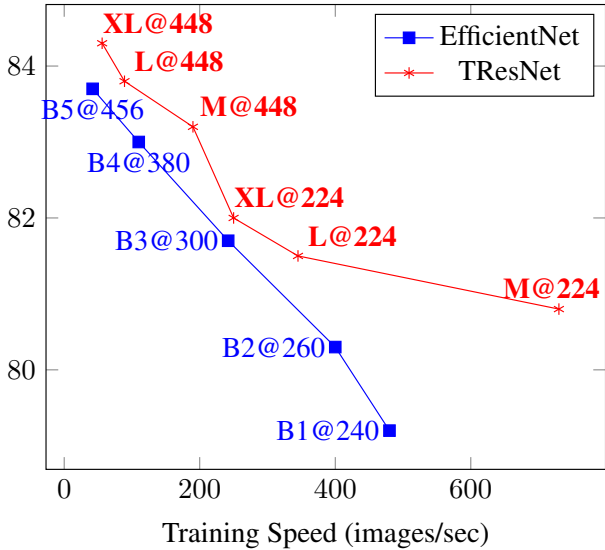


Figure 5. TResNet Vs EfficientNet models training speed comparison. Y label is the accuracy[%]

We can see from Figure 4 and Figure 5 that all along the top-1 accuracy curve, TResNet models give better inference-speed-accuracy and training-speed-accuracy tradeoff than EfficientNet models. Note that each EfficientNet model was bundled and optimized to a specific resolution, while TResNet models were trained and tested on multi-resolutions, which makes this comparison biased to-

ward EfficientNet models; Yet, TResNet models show superior results. Also note that EfficientNet models were trained for 450 epochs and not for 300 epochs like TResNet models, and that EfficientNet training procedure included more GPU intensive tricks (RMSProp optimizer, drop-block) [35], so the actual gap in training times is even higher than stated in Figure 5.

4. Transfer Learning Results

In this section, we will present transfer learning results of TResNet models on four well-known single-label classification downstream datasets. We will also present transfer learning results on multi-label classification and object detection tasks.

4.1. Single-Label Classification

We evaluated TResNet on four commonly used, competitive transfer learning datasets: Stanford-cars [14], CIFAR-10 [15], CIFAR-100 [15] and Oxford-Flowers [27]. For each dataset, we used ImageNet pre-trained checkpoints, and fine-tuned the models for 80 epochs using 1-cycle policy [33]. For the fine-grained classification tasks (Stanford-cars and Oxford-Flowers), in addition to cross-entropy loss we used weighted triplet loss with soft-margin [30, 17], which emphasizes hard examples by focusing of the most difficult positives and negatives samples in the batch. Table 6 shows the transfer learning performance of TResNet, compared to the known state-of-the-art models.

Dataset	Model	Top-1 Acc.	Speed img/sec	Input
CIFAR-10	Gpipe	99.0	-	480
	TResNet-XL	99.0	1060	224
CIFAR-100	EfficientNet-B7	91.7	70	600
	TResNet-XL	91.5	1060	224
Stanford Cars	EfficientNet-B7	94.7	70	600
	TResNet-L	96.0	500	368
Oxford-Flowers	EfficientNet-B7	98.8	70	600
	TResNet-L	99.1	500	368

Table 6. Comparison of TResNet to state-of-the-art models on transfer learning datasets (only ImageNet-based transfer learning results). Models inference speed is measured on a mixed precision V100 GPU. Since no official implementation of Gpipe was provided, its inference speed is unknown.

We can see from Table 6 that TResNet surpasses or matches the state-of-the-art accuracy on 3 of the 4 datasets, with x8-15 faster GPU inference speed. Note that all TResNet’s results are from single-crop single-model evaluation.

4.2. Multi-Label Classification

For multi-label classification experiments, we chose to work with MS-COCO dataset [21] (multi-label recognition task). We used the 2014 split, which contains about 82K images for training and 41K for validation. In total, images are involved with 80 object labels, with an average of 2.9 labels per image.

Our training scheme is similar to the one used for single-label training. The main difference is the loss function, which is adapted for a multi-label settings - we implemented a variant of the well known focal-loss [20], where two different gamma values are used for positive and negative sample. This enables to better tackle the highly imbalanced nature of a multi-label dataset.

Following conventional settings [3, 38], we report the main performance evaluation metric, mean average precision (mAP), but in addition state average per-class precision (CP), recall (CR), F1 (CF1) and the average overall precision (OP), recall (OR), F1 (OF1).

In Table 8, we present the transfer learning results of TResNet model and compare it to the known state-of-the-art model.

Backbone	mAP	CP	CR	CF1	OP	OR	OF1
KSSNet[38]	83.7	84.6	73.2	77.2	87.8	76.2	81.5
LTResNet	88.0	88.4	77.3	82.5	88.7	80.0	84.1

Table 8. **Comparison of TResNet to state-of-the-art model on multi-label classification on MS-COCO dataset.** KSSNet [38], is the known SOTA, based on ResNet101 backbone.

We can see from Table 8 that the TResNet-based solution significantly outperforms previous top solution for MS-COCO multi-label dataset, increasing the known SOTA from 83.7 mAP to 88.0 mAP. All additional evaluation metrics also show improvement.

4.3. Object Detection

While our main focus was on various classification tasks, we wanted to further test TResNet on another popular computer vision task - object detection.

We used the known MS-COCO [21] dataset (object detection task), with a training set with 118k images, and an evaluation set (minival) of 5k images. For training, we used the popular mm-detection [2] package, with FCOS [37] as the object detection method and the enhancements discussed in ATSS [45].

We trained with SGD optimizer for 70 epochs with 0.9 momentum and weight decay of 0.0001. We used learning rate warm up, initial learning rate of 0.01 and 10x reduction at epochs 40, 60. We also implemented the data augmentations techniques described in [22].

For a fair comparison, we used first ResNet50 as backbone, and then replace it by MTResNet (both models give similar GPU throughput). Comparison results appear in Table 9.

Method	Babkbone	mAP %
FCOS	ResNet50	42.8
FCOS	MTResNet	44.0

Table 9. **Comparison of MTResNet to ResNet50 on MS-COCO object detection task.** Results were obtained using mm-detection package, with FCOS as the object detection method .

We can see from Table 9 that MTResNet outperform ResNet50 on object-detection task, increasing COCO mAP score from 42.8 to 44.0. This is consistent with the improvement we saw in single-label ImageNet classification task.

5. Conclusion

In this paper, we point out a possible blind-spot of latest developments in neural network design patterns. They tend not to consider actual GPU utilization as one of the measurements for a network quality. While GPU inference speed is sometimes measured, GPU training speed and maximal possible batch size are widely overlooked. For many real-world deep learning applications, training speed, inference speed and maximal batch size are all critical factors.

To address this issue, we propose a carefully selected set of design refinements, which are highly effective in utilizing typical GPU resources - SpaceToDepth stem cell, economical AA downsampling, Inplace-ABN operations, block-type selection redesign and optimized SE layers. We combine these refinements with a serious of code optimizations and enhancements to suggest a family of new models, dedicated for GPU high-performance, which we call TResNet.

We demonstrate that on ImageNet, all along the top-1 accuracy curve TResNet gives better GPU throughput than existing models. In addition, on four commonly used downstream single-label classification datasets it reaches new state-of-the-art accuracies. We also show that TResNet generalizes well to other computer vision tasks, reaching top scores on multi-label classification and object detection datasets.

References

- [1] Han Cai, Ligeng Zhu, and Song Han. Proxylesnas: Direct neural architecture search on target task and hardware. *arXiv preprint arXiv:1812.00332*, 2018.
- [2] Kai Chen, Jiaqi Wang, Jiangmiao Pang, Yuhang Cao, Yu Xiong, Xiaoxiao Li, Shuyang Sun, Wansen Feng, Ziwei Liu,

- Jiarui Xu, Zheng Zhang, Dazhi Cheng, Chenchen Zhu, Tianheng Cheng, Qijie Zhao, Buyu Li, Xin Lu, Rui Zhu, Yue Wu, Jifeng Dai, Jingdong Wang, Jianping Shi, Wanli Ouyang, Chen Change Loy, and Dahua Lin. MMDetection: Open mmlab detection toolbox and benchmark. *arXiv preprint arXiv:1906.07155*, 2019.
- [3] Zhao-Min Chen, Xiu-Shen Wei, Peng Wang, and Yanwen Guo. Multi-label image recognition with graph convolutional networks, 2019.
- [4] Ekin D Cubuk, Barret Zoph, Dandelion Mane, Vijay Vasudevan, and Quoc V Le. Autoaugment: Learning augmentation strategies from data. In *Proceedings of the IEEE conference on computer vision and pattern recognition*, pages 113–123, 2019.
- [5] Terrance DeVries and Graham W Taylor. Improved regularization of convolutional neural networks with cutout. *arXiv preprint arXiv:1708.04552*, 2017.
- [6] Shanghua Gao, Ming-Ming Cheng, Kai Zhao, Xin-Yu Zhang, Ming-Hsuan Yang, and Philip HS Torr. Res2net: A new multi-scale backbone architecture. *IEEE transactions on pattern analysis and machine intelligence*, 2019.
- [7] Kaiming He, Haoqi Fan, Yuxin Wu, Saining Xie, and Ross Girshick. Momentum contrast for unsupervised visual representation learning, 2019.
- [8] Kaiming He, Xiangyu Zhang, Shaoqing Ren, and Jian Sun. Deep residual learning for image recognition. In *Proceedings of the IEEE conference on computer vision and pattern recognition*, pages 770–778, 2016.
- [9] Tong He, Zhi Zhang, Hang Zhang, Zhongyue Zhang, Junyuan Xie, and Mu Li. Bag of tricks for image classification with convolutional neural networks. In *Proceedings of the IEEE Conference on Computer Vision and Pattern Recognition*, pages 558–567, 2019.
- [10] Andrew Howard, Mark Sandler, Grace Chu, Liang-Chieh Chen, Bo Chen, Mingxing Tan, Weijun Wang, Yukun Zhu, Ruoming Pang, Vijay Vasudevan, et al. Searching for mobilenetv3. In *Proceedings of the IEEE International Conference on Computer Vision*, pages 1314–1324, 2019.
- [11] Jie Hu, Li Shen, and Gang Sun. Squeeze-and-excitation networks. In *Proceedings of the IEEE conference on computer vision and pattern recognition*, pages 7132–7141, 2018.
- [12] Jeremiah W Johnson. Adapting mask-rcnn for automatic nucleus segmentation. *arXiv preprint arXiv:1805.00500*, 2018.
- [13] Alexander Kolesnikov, Lucas Beyer, Xiaohua Zhai, Joan Puigcerver, Jessica Yung, Sylvain Gelly, and Neil Houlsby. Large scale learning of general visual representations for transfer. *arXiv preprint arXiv:1912.11370*, 2019.
- [14] Jonathan Krause, Jia Deng, Michael Stark, and Li Fei-Fei. Collecting a large-scale dataset of fine-grained cars. 2013.
- [15] Alex Krizhevsky, Geoffrey Hinton, et al. Learning multiple layers of features from tiny images. 2009.
- [16] Alex Krizhevsky, Ilya Sutskever, and Geoffrey E Hinton. Imagenet classification with deep convolutional neural networks. In F. Pereira, C. J. C. Burges, L. Bottou, and K. Q. Weinberger, editors, *Advances in Neural Information Processing Systems 25*, pages 1097–1105. Curran Associates, Inc., 2012.
- [17] Hussam Lawen, Avi Ben-Cohen, Matan Protter, Itamar Friedman, and Lihi Zelnik-Manor. Compact network training for person reid. *Proceedings of the 2020 International Conference on Multimedia Retrieval*, Jun 2020.
- [18] Jungkyu Lee, Taeryun Won, and Kiho Hong. Compounding the performance improvements of assembled techniques in a convolutional neural network. *arXiv preprint arXiv:2001.06268*, 2020.
- [19] Zeming Li, Chao Peng, Gang Yu, Xiangyu Zhang, Yangdong Deng, and Jian Sun. Detnet: A backbone network for object detection. *arXiv preprint arXiv:1804.06215*, 2018.
- [20] Tsung-Yi Lin, Priya Goyal, Ross Girshick, Kaiming He, and Piotr Dollr. Focal loss for dense object detection, 2017.
- [21] Tsung-Yi Lin, Michael Maire, Serge Belongie, Lubomir Bourdev, Ross Girshick, James Hays, Pietro Perona, Deva Ramanan, C. Lawrence Zitnick, and Piotr Dollr. Microsoft coco: Common objects in context, 2014.
- [22] Wei Liu, Dragomir Anguelov, Dumitru Erhan, Christian Szegedy, Scott Reed, Cheng-Yang Fu, and Alexander C. Berg. Ssd: Single shot multibox detector. *Lecture Notes in Computer Science*, pages 21–37, 2016.
- [23] Ilya Loshchilov and Frank Hutter. Decoupled weight decay regularization. *arXiv preprint arXiv:1711.05101*, 2017.
- [24] Ningning Ma, Xiangyu Zhang, Hai-Tao Zheng, and Jian Sun. Shufflenet v2: Practical guidelines for efficient cnn architecture design. In *Proceedings of the European Conference on Computer Vision (ECCV)*, pages 116–131, 2018.
- [25] Stefano Markidis, Steven Wei Der Chien, Erwin Laure, Ivy Bo Peng, and Jeffrey S Vetter. Nvidia tensor core programmability, performance & precision. In *2018 IEEE International Parallel and Distributed Processing Symposium Workshops (IPDPSW)*, pages 522–531. IEEE, 2018.
- [26] Diganta Misra. Mish: A self regularized non-monotonic neural activation function, 2019.
- [27] Maria-Elena Nilsback and Andrew Zisserman. Automated flower classification over a large number of classes. In *2008 Sixth Indian Conference on Computer Vision, Graphics & Image Processing*, pages 722–729. IEEE, 2008.
- [28] Adam Paszke, Sam Gross, Soumith Chintala, Gregory Chanan, Edward Yang, Zachary DeVito, Zeming Lin, Alban Desmaison, Luca Antiga, and Adam Lerer. Automatic differentiation in pytorch. 2017.
- [29] Adam Paszke, Sam Gross, Francisco Massa, Adam Lerer, James Bradbury, Gregory Chanan, Trevor Killeen, Zeming Lin, Natalia Gimeshein, Luca Antiga, et al. Pytorch: An imperative style, high-performance deep learning library. In *Advances in Neural Information Processing Systems*, pages 8024–8035, 2019.
- [30] Ergys Ristani and Carlo Tomasi. Features for multi-target multi-camera tracking and re-identification. In *Proceedings of the IEEE conference on computer vision and pattern recognition*, pages 6036–6046, 2018.
- [31] Samuel Rota Bulò, Lorenzo Porzi, and Peter Kontschieder. In-place activated batchnorm for memory-optimized training of dnns. In *Proceedings of the IEEE Conference on Computer Vision and Pattern Recognition*, 2018.

- [32] Mark Sandler, Jonathan Baccash, Andrey Zhmoginov, and Andrew Howard. Non-discriminative data or weak model? on the relative importance of data and model resolution. *arXiv preprint arXiv:1909.03205*, 2019.
- [33] Leslie N Smith. A disciplined approach to neural network hyper-parameters: Part 1—learning rate, batch size, momentum, and weight decay. *arXiv preprint arXiv:1803.09820*, 2018.
- [34] Christian Szegedy, Vincent Vanhoucke, Sergey Ioffe, Jonathon Shlens, and Zbigniew Wojna. Rethinking the inception architecture for computer vision. *CoRR*, abs/1512.00567, 2015.
- [35] Mingxing Tan and Quoc V Le. Efficientnet: Rethinking model scaling for convolutional neural networks. *arXiv preprint arXiv:1905.11946*, 2019.
- [36] Mingxing Tan and Quoc V Le. Mixnet: Mixed depthwise convolutional kernels. *arXiv preprint arXiv:1907.09595*, 2019.
- [37] Zhi Tian, Chunhua Shen, Hao Chen, and Tong He. Fcos: Fully convolutional one-stage object detection, 2019.
- [38] Ya Wang, Dongliang He, Fu Li, Xiang Long, Zhichao Zhou, Jinwen Ma, and Shilei Wen. Multi-label classification with label graph superimposing. *ArXiv*, abs/1911.09243, 2019.
- [39] Ross Wightman. `pytorch-image-models`, 2019. <https://github.com/rwightman/pytorch-image-models>.
- [40] Bin Xiao, Haiping Wu, and Yichen Wei. Simple baselines for human pose estimation and tracking. In *Proceedings of the European conference on computer vision (ECCV)*, pages 466–481, 2018.
- [41] Saining Xie, Ross Girshick, Piotr Dollár, Zhuowen Tu, and Kaiming He. Aggregated residual transformations for deep neural networks. In *Proceedings of the IEEE conference on computer vision and pattern recognition*, pages 1492–1500, 2017.
- [42] Rengan Xu, Frank Han, and Quy Ta. Deep learning at scale on nvidia v100 accelerators. In *2018 IEEE/ACM Performance Modeling, Benchmarking and Simulation of High Performance Computer Systems (PMBS)*, pages 23–32. IEEE, 2018.
- [43] Masafumi Yamazaki, Akihiko Kasagi, Akihiro Tabuchi, Takumi Honda, Masahiro Miwa, Naoto Fukumoto, Tsuguchika Tabaru, Atsushi Ike, and Kohta Nakashima. Yet another accelerated sgd: Resnet-50 training on imagenet in 74.7 seconds. *arXiv preprint arXiv:1903.12650*, 2019.
- [44] Richard Zhang. Making convolutional networks shift-invariant again. In *ICML*, 2019.
- [45] Shifeng Zhang, Cheng Chi, Yongqiang Yao, Zhen Lei, and Stan Z. Li. Bridging the gap between anchor-based and anchor-free detection via adaptive training sample selection, 2019.

Appendices

A. Code for Different Modules in TResNet

JIT accelerated SpaceToDepth module

```
@torch.jit.script
class SpaceToDepthJIT(object):
    def __call__(self, x: torch.Tensor):
        N, C, H, W = x.size()
        x = x.view(N, C, H // 4, 4, W // 4, 4)
        x = x.permute(0, 3, 5, 1, 2, 4).contiguous()
        x = x.view(N, C * 16, H // 4, W // 4)
        return x
```

JIT accelerated AA downsampling module

```
@torch.jit.script
class AADownsamplingJIT(object):
    def __init__(self, channels: int, mixed_precision: bool = True):
        a = torch.tensor([1., 2., 1.])
        filt = (a[:, None] * a[None, :]).clone().detach()
        filt = filt / torch.sum(filt)
        self.filt = filt[None, None, :, :].repeat((channels, 1, 1, 1))
        self.filt = self.filt.cuda()
        if mixed_precision:
            self.filt = self.filt.half()

    def __call__(self, input: torch.Tensor):
        input_pad = F.pad(input, (1, 1, 1, 1), 'reflect')
        return F.conv2d(input_pad, self.filt, stride=2,
                        padding=0, groups=input.shape[1])
```

Fast implementation of global average pooling

```
class FastGlobalAvgPool2d():
    def __init__(self, flatten=False):
        self.flatten = flatten

    def __call__(self, x):
        if self.flatten:
            in_size = x.size()
            return x.view((in_size[0], in_size[1], -1)).mean(dim=2)
        else:
            return x.view(x.size(0), x.size(1), -1).mean(-1).view(
                x.size(0), x.size(1), 1, 1)
```